Supplementary Information

Anomalous Reverse Mechanical Polarization Switching In Negative Piezoelectric $CuInP_2S_6$

Lei Wang[1#], Dawei Zhang[1,2#], Zheng-Dong Luo[3,4], Patrick D. Taylor[5], Kevin Tran[5], Wenjie Ming[6,7], Jianbo Tang[8], Pankaj Sharma[9,10,2], Michelle J.S. Spencer[11], Jan Seidel[1,2*]

[1]School of Materials Science and Engineering, UNSW Sydney, Sydney NSW 2052, Australia

[2]ARC Centre of Excellence in Future Low-Energy Electronics Technologies (FLEET), UNSW Sydney, Sydney NSW 2052, Australia

[3]Hangzhou Institute of Technology, Xidian University, Hangzhou 311200, China

[4]State Key Discipline Laboratory of Wide Band Gap Semiconductor Technology, School of Microelectronics, Xidian University, Xi'an 710071, P. R. China

[5]School of Science, RMIT University, GPO Box 2476, Melbourne, Victoria 3001, Australia

[6]Department of Materials Science and Engineering, Southern University of Science and Technology, Shenzhen, Guangdong 518055, China

[7]Guangdong Provincial Key Laboratory of Functional Oxide Materials and Devices, Southern University of Science and Technology, Shenzhen, Guangdong 518055, China

[8]School of Chemical Engineering, UNSW Sydney, Sydney NSW 2052, Australia

[9]College of Science and Engineering, Flinders University, Bedford Park, Adelaide, SA 5042, Australia.

[10]Flinders Institute for Nanoscale Science and Technology, Flinders University, Adelaide, SA 5042, Australia

[11]ARC Centre of Excellence in Future Low-Energy Electronics Technologies, School of Science, RMIT University, GPO Box 2476, Melbourne, Victoria 3001, Australia

[#]These authors contribute equally

*correspondence: jan.seidel@unsw.edu.au

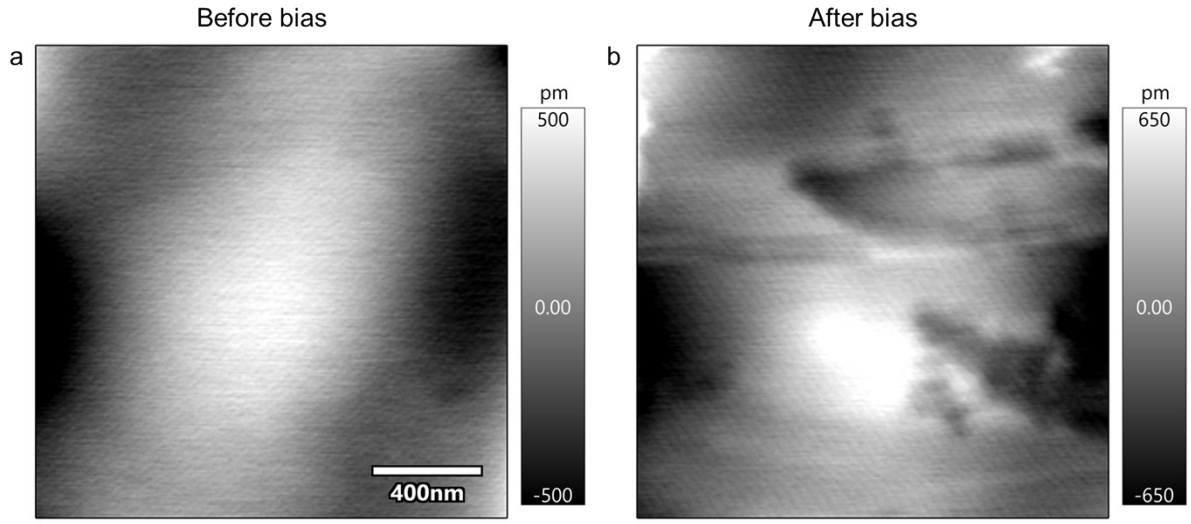

Figure S1. Surface damage caused by the electric field. (a) Morphology of the initial state, (b) morphology after the application of tip bias.

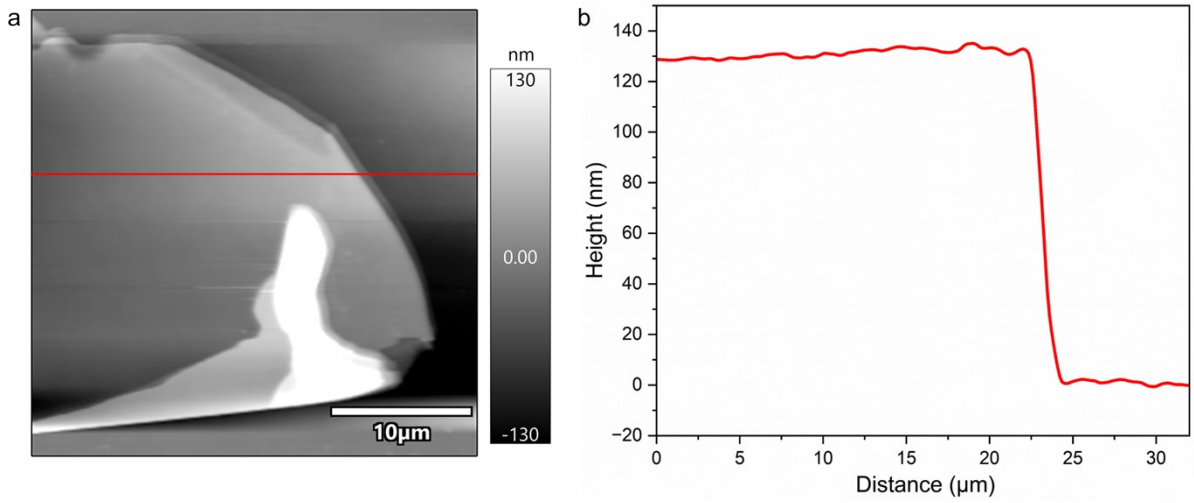

Figure S2. Thickness of the CIPS nanoflake. (a) Morphology of the CIPS nanoflake, (b) corresponding height profile of the red line denoted in (a).

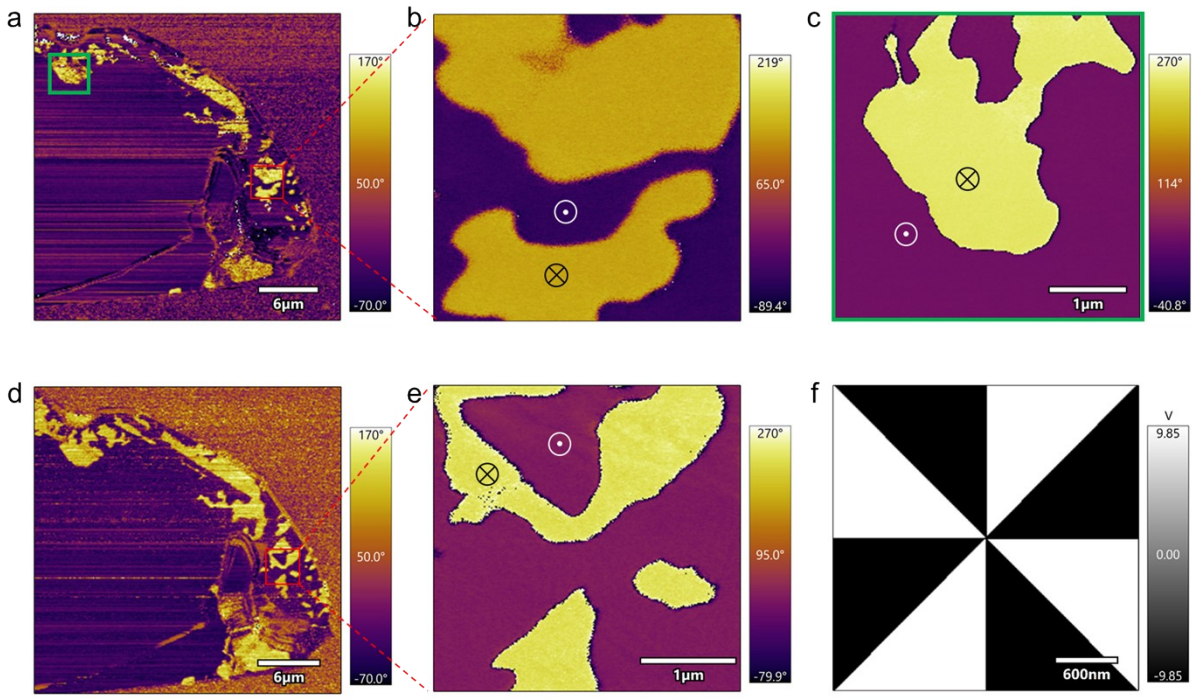

Figure S3. Polarization direction determination. (a) Phase map of the CIPS nanoflake, (b) phase map of the red square area in (a), which is also the area exhibited in the Main text Figure 2, (c) phase map of the green square area in (a), which is also the area exhibited in Figure S12. (d) Phase map of the same CIPS nanoflake after electrical writing in the red square, (e) phase map of the red square area in (d), where electric bias applied, (f) the pattern of the applied electric bias.

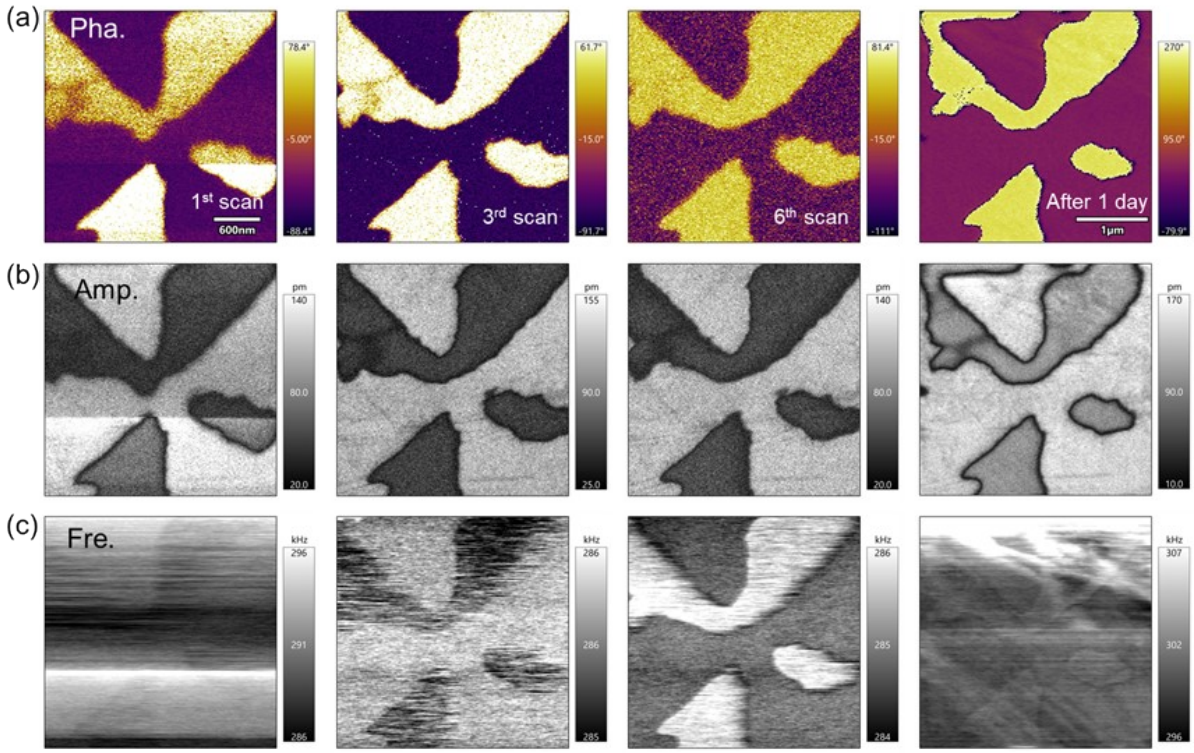

Figure S4. Charge injection effect. (a) Phase maps directly after electrical writing (1st scan, 3rd scan and 6th scan) and after 1 day, (b) corresponding amplitude maps, (c) corresponding phase maps.

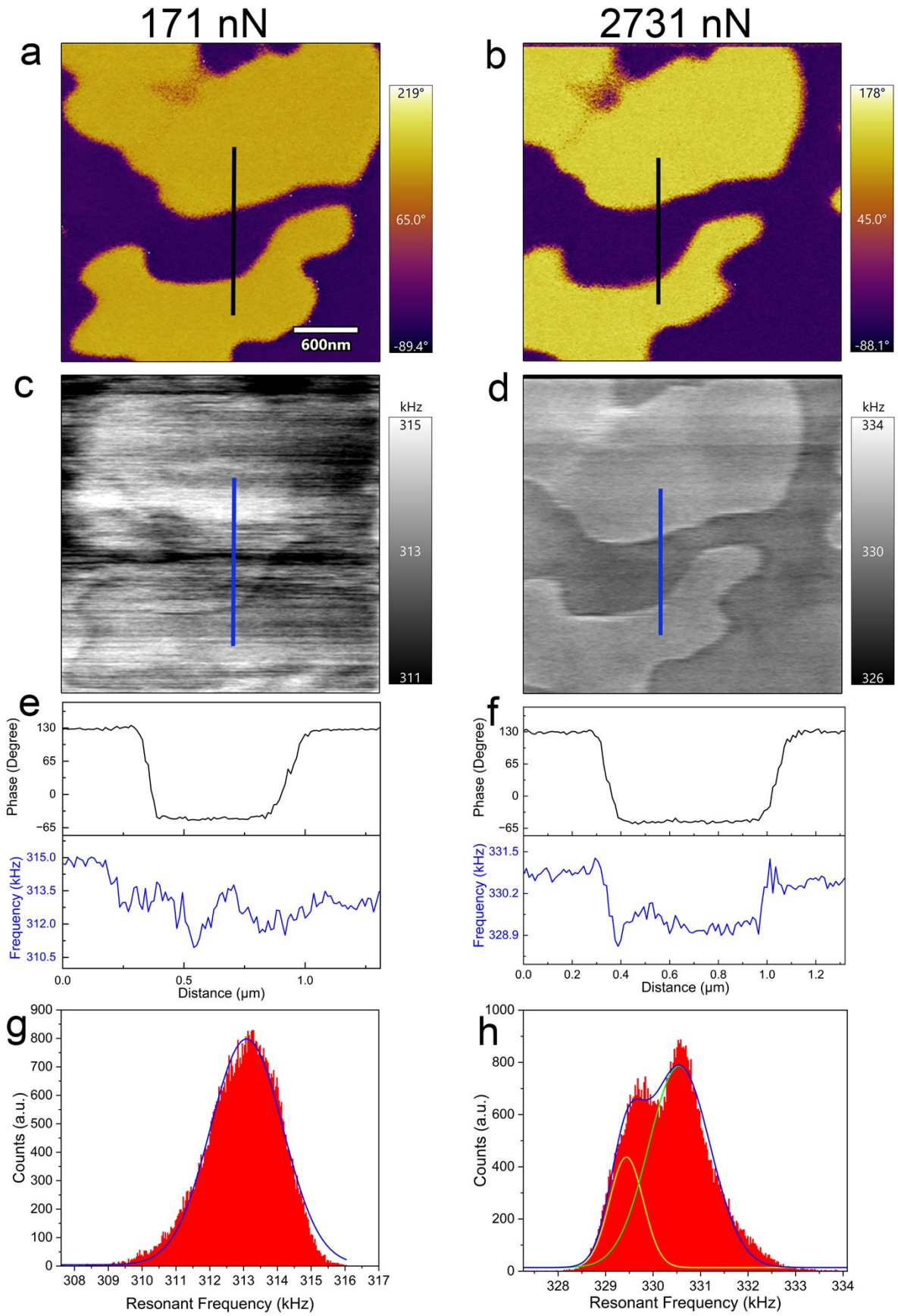

Figure S5. Flexoelectric effect on mechanical properties of CIPS. (a,b) Phase maps which contain upward (purple) and downward (yellow) domains, (c.,d) corresponding resonant

frequency maps by DART-PFM under low (171 nN) and high (2731 nN) tip forces. (e,f) Vertical line cut (average over 20 lines) along the black and blue lines in the image (a-d), respectively. (g,h) Histogram corresponding to the resonant frequency maps in (c,d), respectively.

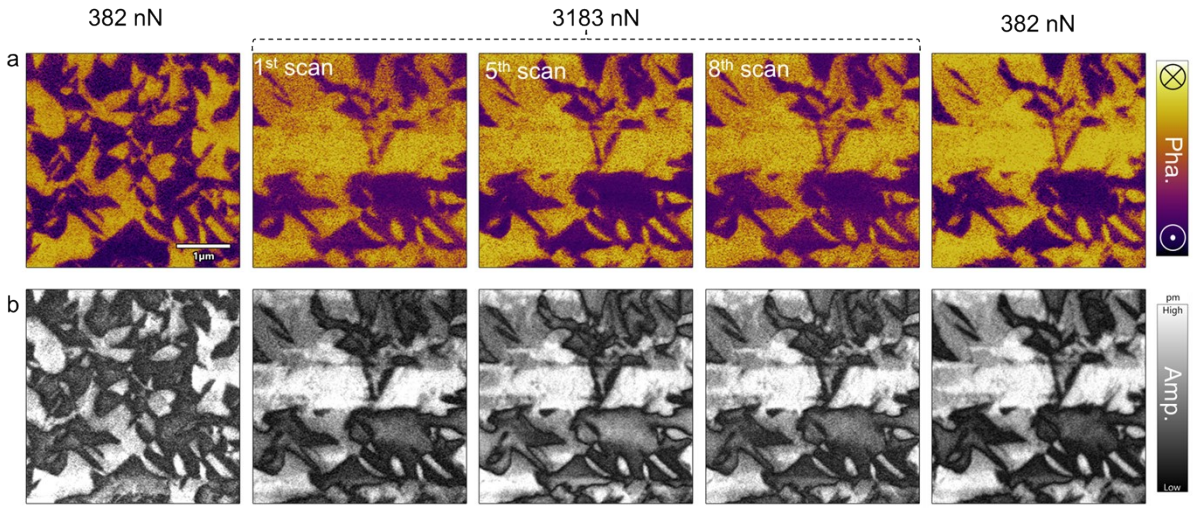

Figure S6. Mechanical polarization switching in PMN-PT single crystal. (a) Phase maps which contain both upward domains (purple) and downward domains (yellow) before high tip force, during high tip force and after high tip force, (b) corresponding amplitude maps.

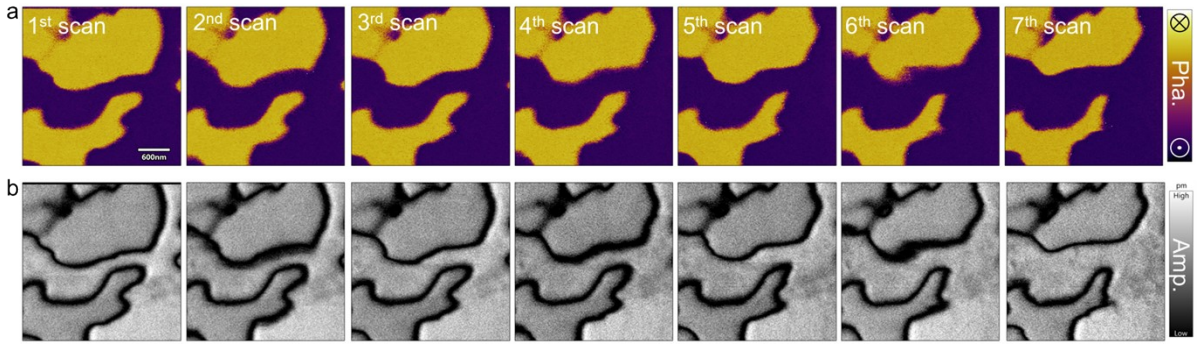

Figure S7. Domain evolution under high tip force. (a) Phase maps with increased force cycles, (b) corresponding amplitude maps.

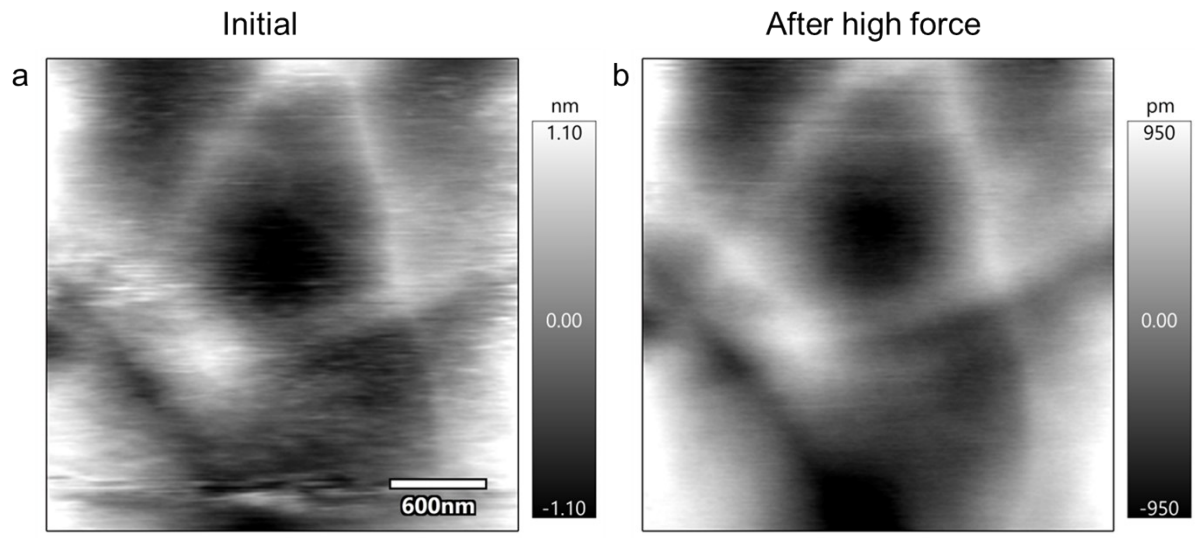

Figure S8. Surface before and after mechanical writing. (a) Morphology of initial state, (b) morphology after the application of high tip force.

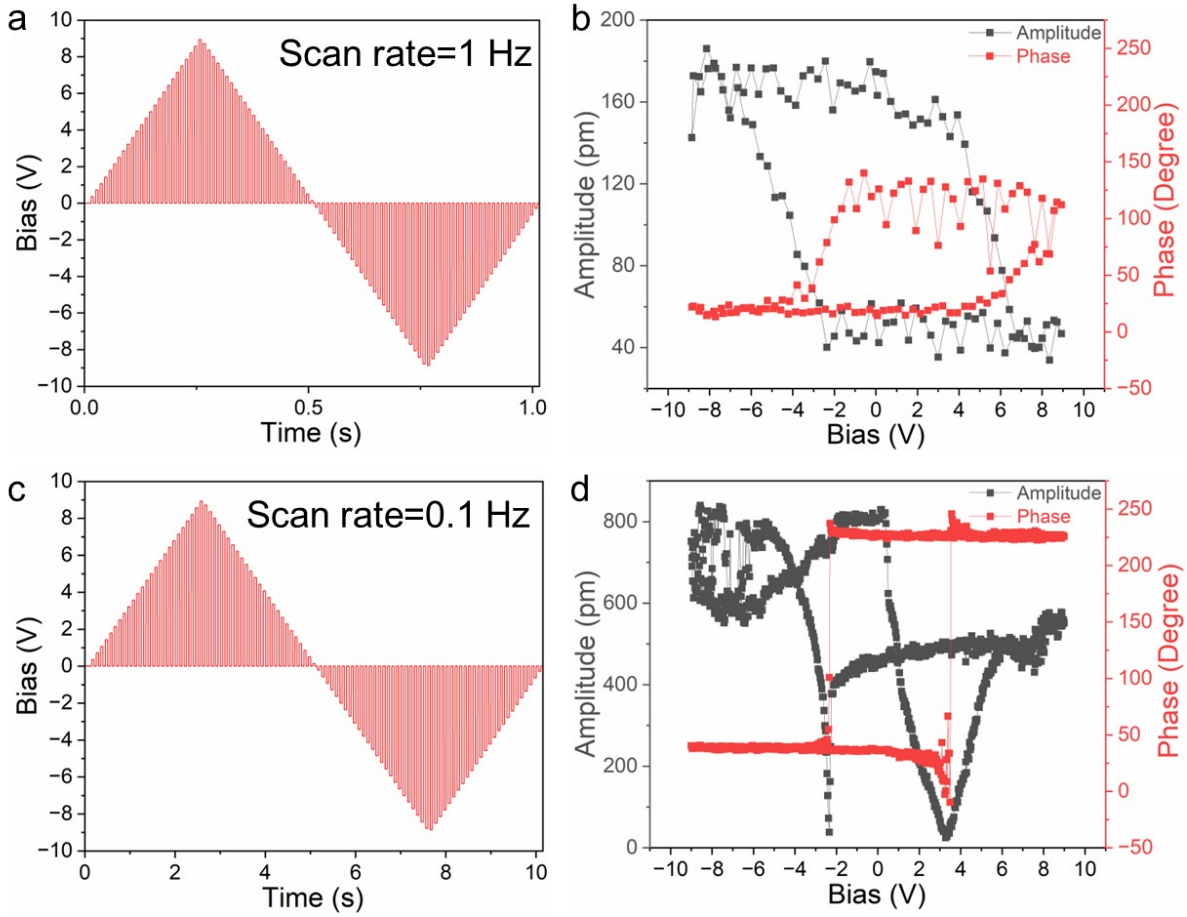

Figure S9. Time-dependent hysteresis loop. (a) Trianglesquare bias of the 1-Hz scan rate, (b) corresponding SSPFM loop. (c) Trianglesquare bias of the 0.1-Hz scan rate, (d) corresponding SSPFM loop.

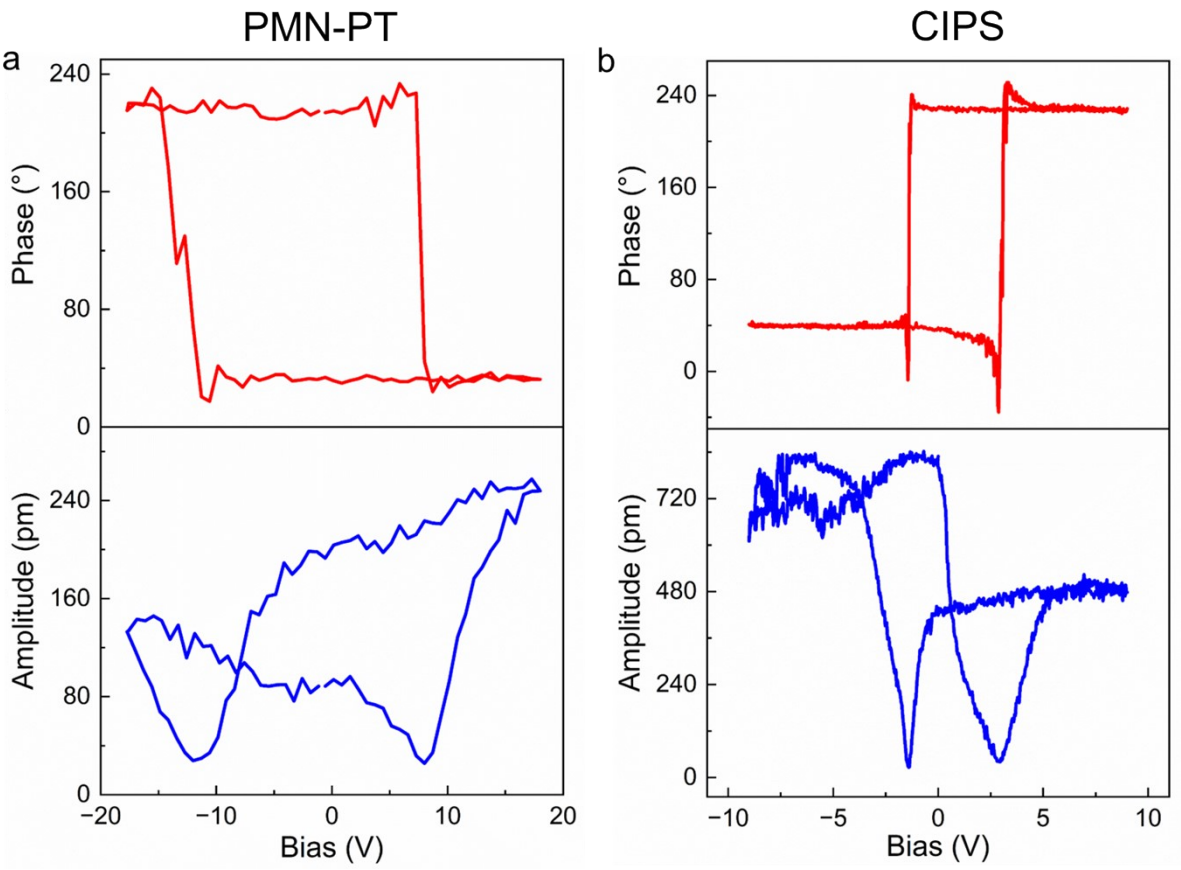

Figure S10. PFM phase (top panel) and amplitude (bottom panel) loops. (a) PMN-PT. (b) CIPS.

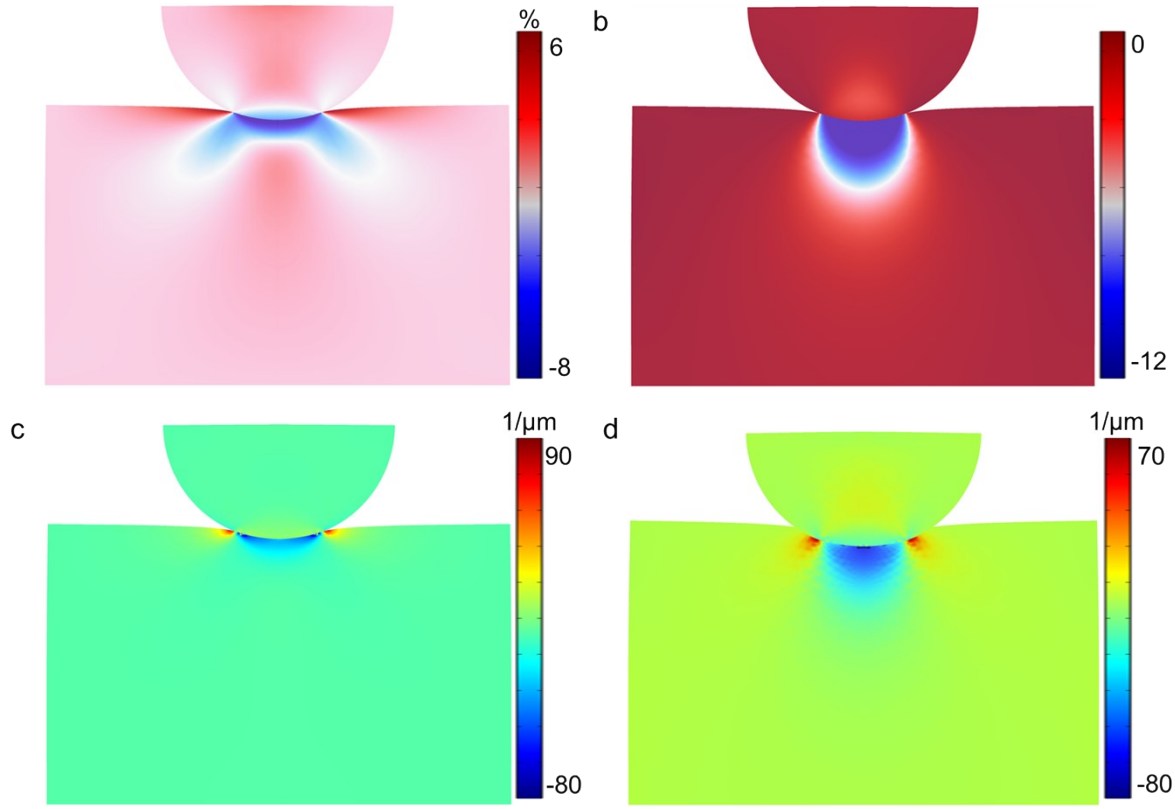

Figure S11. Strain and strain gradients under tip pressure of 2731 nN. (a) Strain ε_{rr}, (b) strain ε_{zz}. (c) Strain gradient $\varepsilon_{rr,z}$, (d) strain gradient $\varepsilon_{zz,z}$.

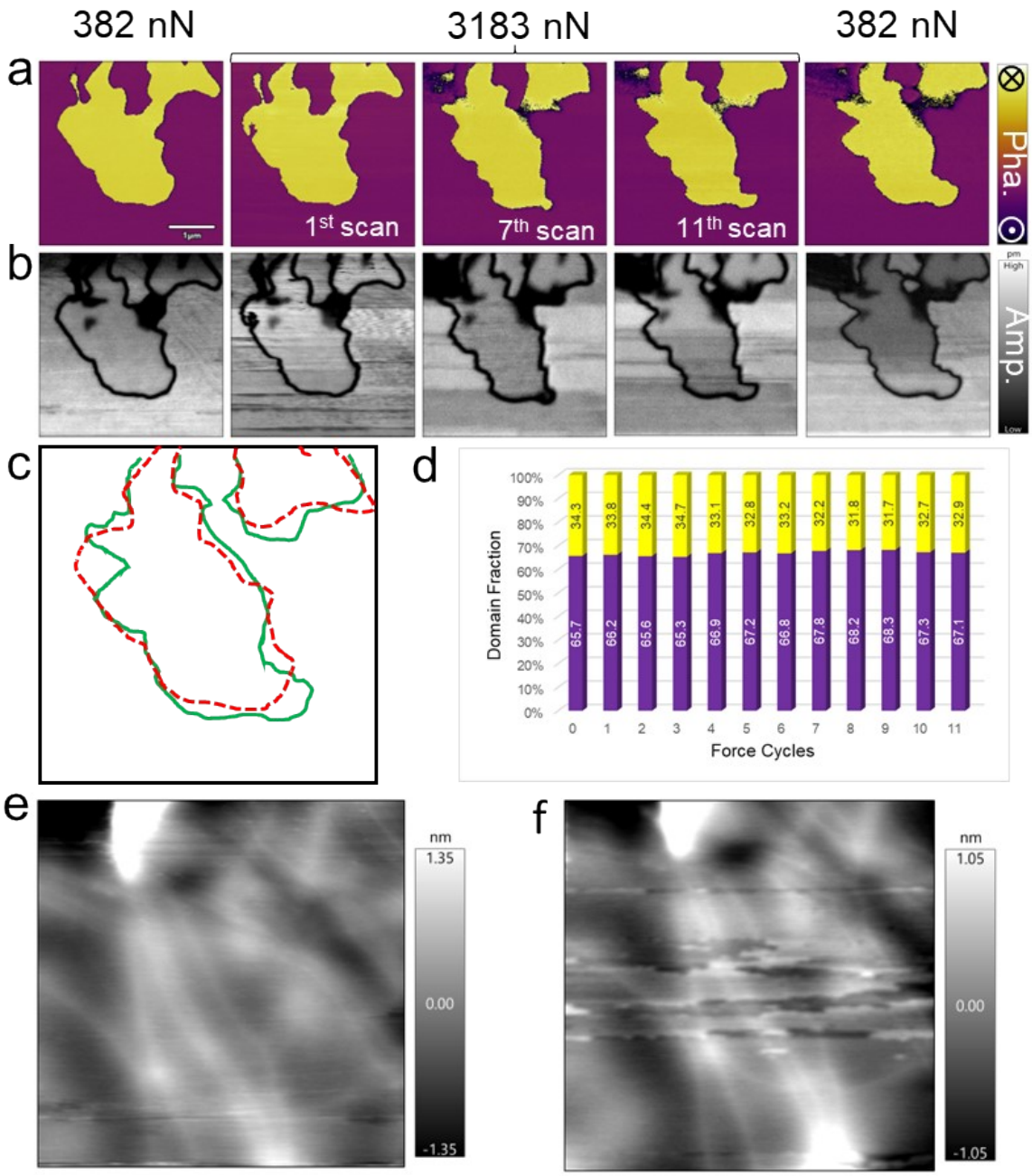

Figure S12. Bidirectional mechanical polarization switching in CIPS. (a) Phase maps which contain both upward domains (purple) and downward domains (yellow) before high tip force, during high tip force and after high tip force, (b) corresponding amplitude maps. (c) Schematic of domain walls before (red dash lines) and after (green solid lines) mechanical switching. (d) Domain fraction evolution with increased force cycles. (e) Morphology before mechanical writing, (f) corresponding morphology after mechanical writing.

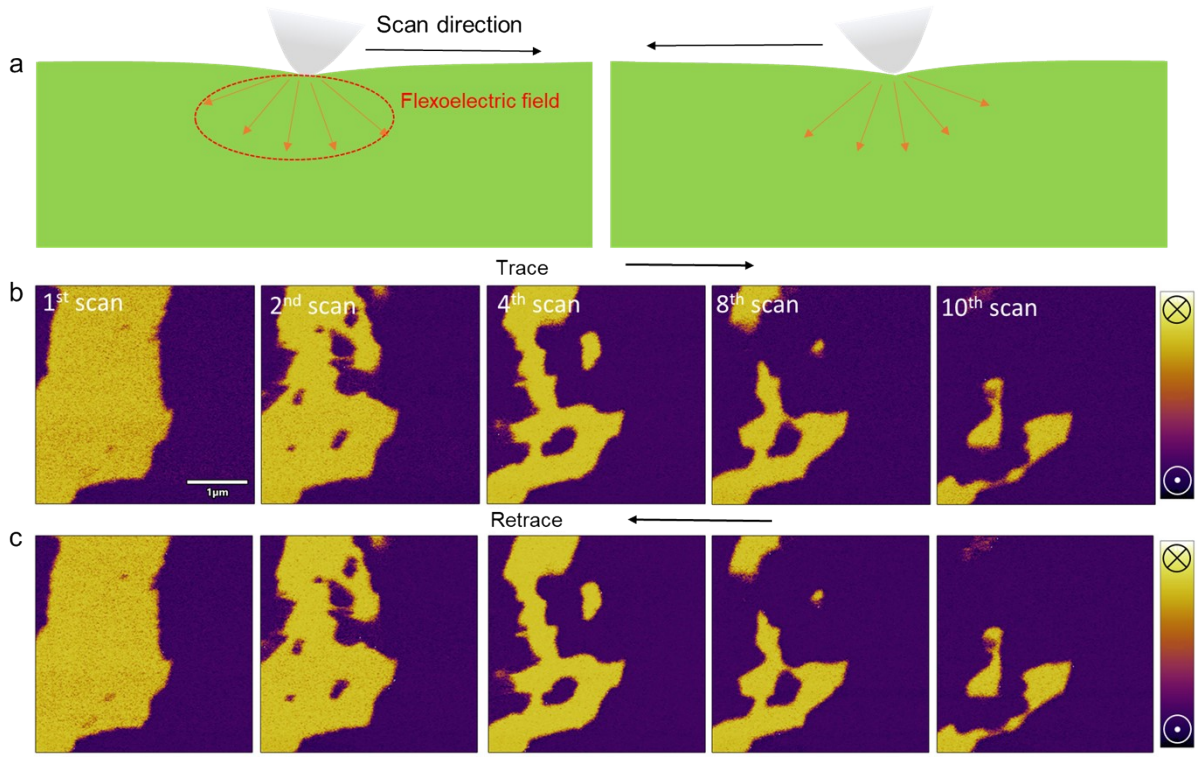

Figure S13. Domain evolution during both trace and retrace processes. (a) Schematic of asymmetric flexoelectric field during trace (scanning from left to right) and retrace (scanning from right to left) processes. (b) PFM phase maps during trace process under high tip force, (c) corresponding phase maps during retrace process.

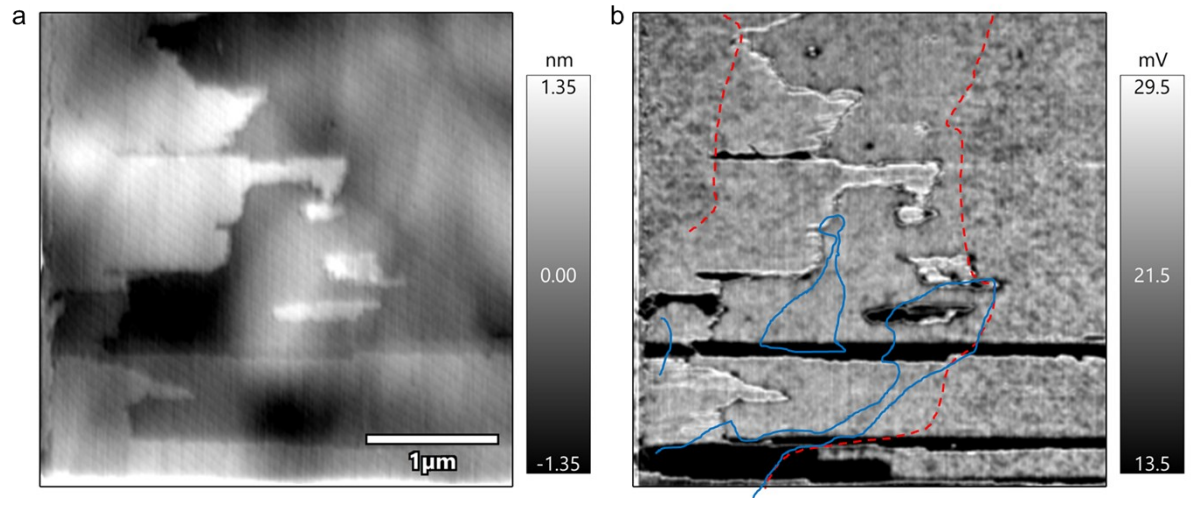

Figure S14. Friction behaviour after mechanical writing. (a) Morphology which is the same area in Figure S13, (b) corresponding friction map detected after mechanical writing, in which red dash line and blue solid line are the domain walls before and after mechanical writing, respectively.

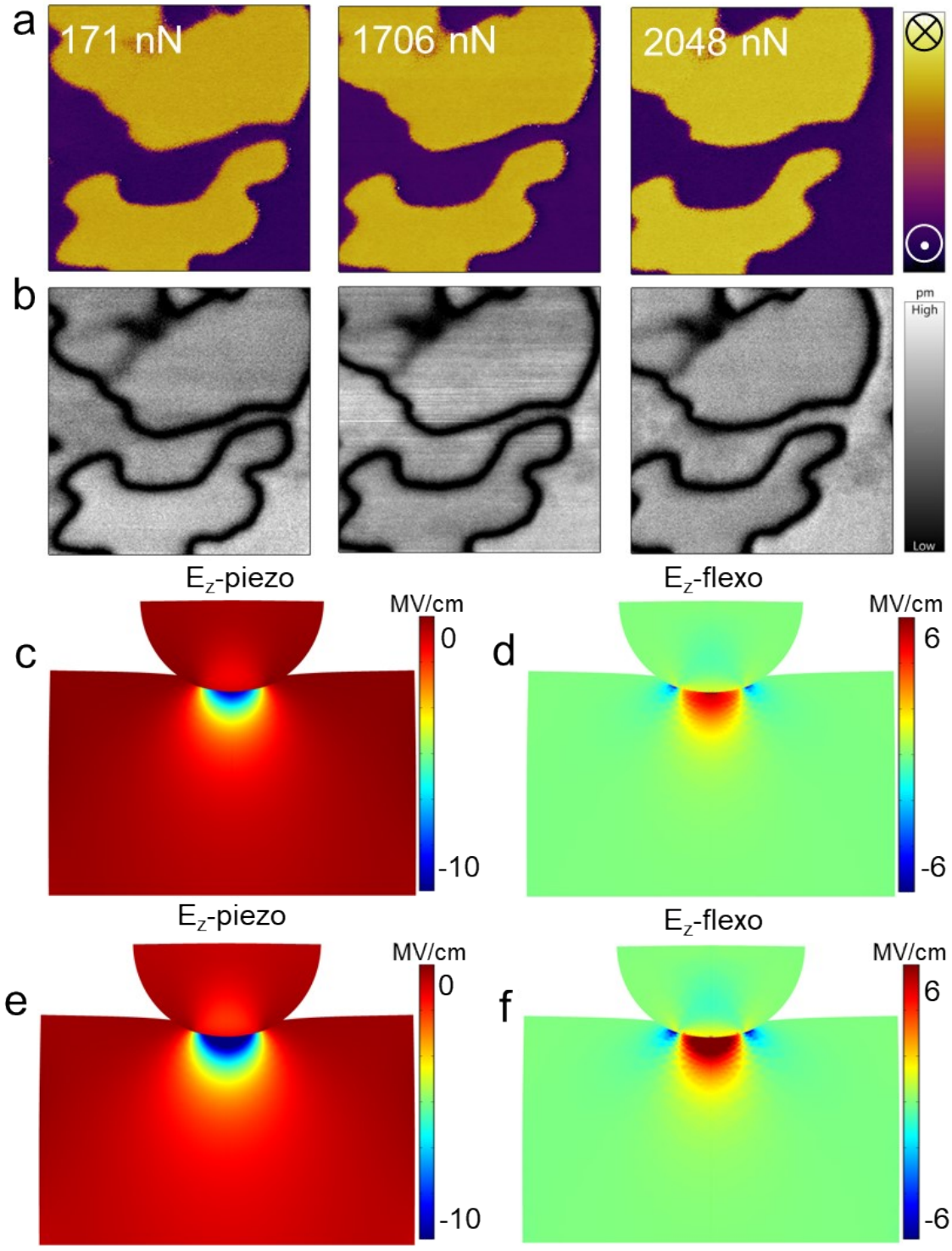

Figure S15. Threshold force for mechanical polarization switching in both experiment and calculation results. (a) Phase maps under different tip forces, (b) corresponding amplitude maps. (c) Piezoelectric field under 1706-nN tip force, (d) corresponding flexoelectric field. (e) Piezoelectric field under 2048-nN tip force, (d) corresponding flexoelectric field.

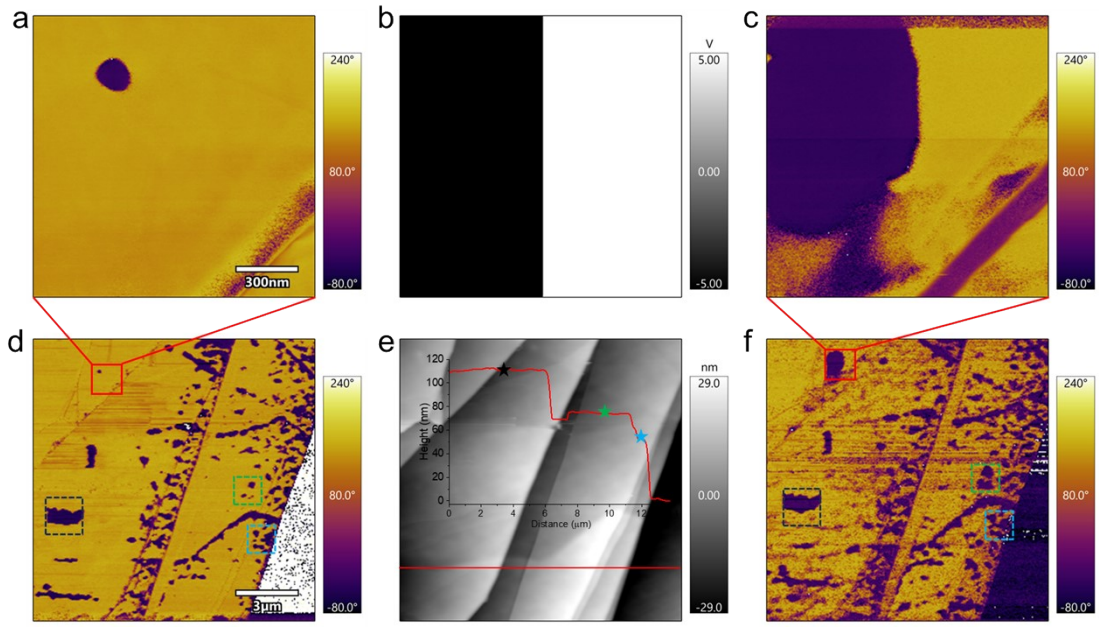

Figure S16. Characterization of polarization direction and CIPS thickness. (a) The phase map before electric writing. (b) Electric bias applied. (c) The phase map after electric writing. (d) Large-area phase map before electric and mechanical writing, and the red square area indicates the area shown in (a). (e) Morphology map. The inset exhibits the height profile of the red line. (f) Large-area phase map after electric and mechanical writing, and the red square area indicates the area shown in (c).

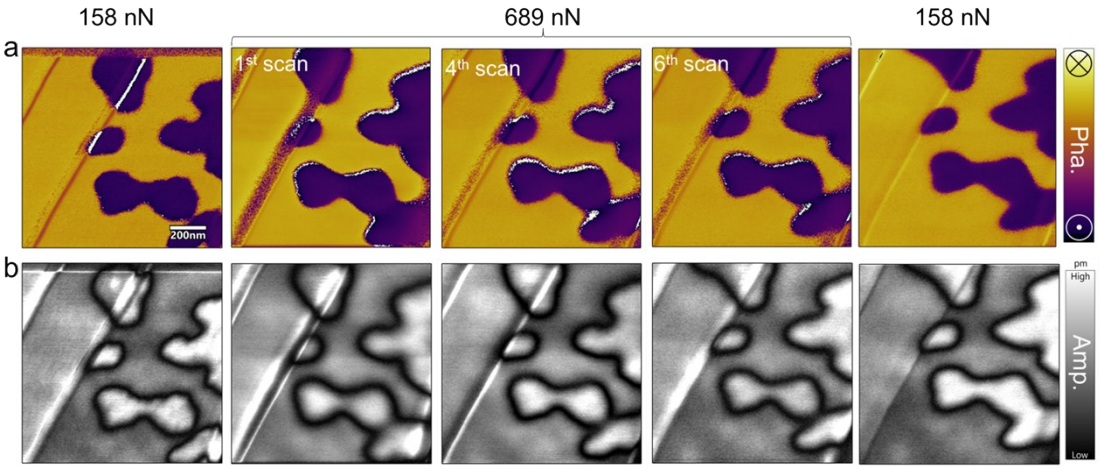

Figure S17. Anomalous mechanical polarization switching in 50-nm CIPS, which has been labelled by the blue square in Figure S16. (a) Phase maps which contain both upward domains (purple) and downward domains (yellow) before high tip force, during high tip force, and after high tip force, (b) corresponding amplitude maps.

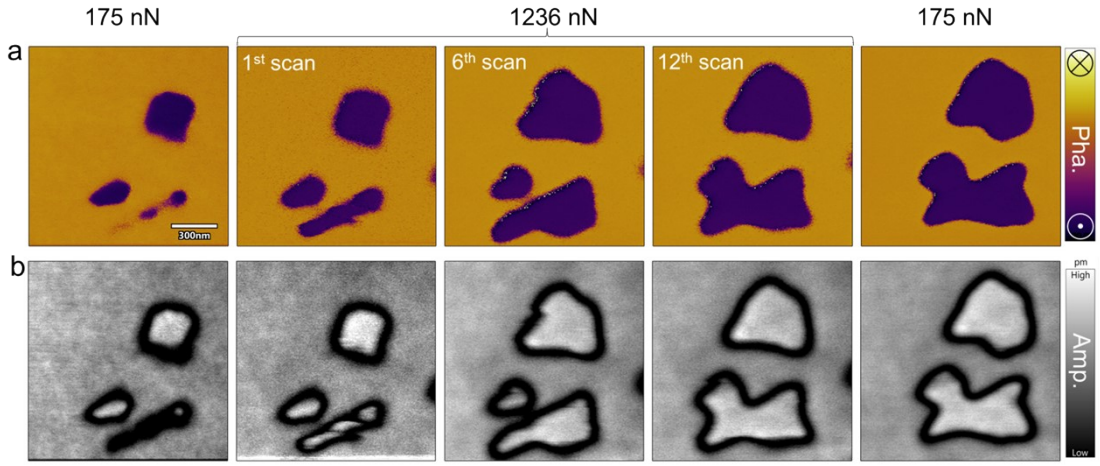

Figure S18. Anomalous mechanical polarization switching in 72-nm CIPS, which has been labelled by the green square in Figure S16. (a) Phase maps which contain both upward domains (purple) and downward domains (yellow) before high tip force, during high tip force, and after high tip force, (b) corresponding amplitude maps.

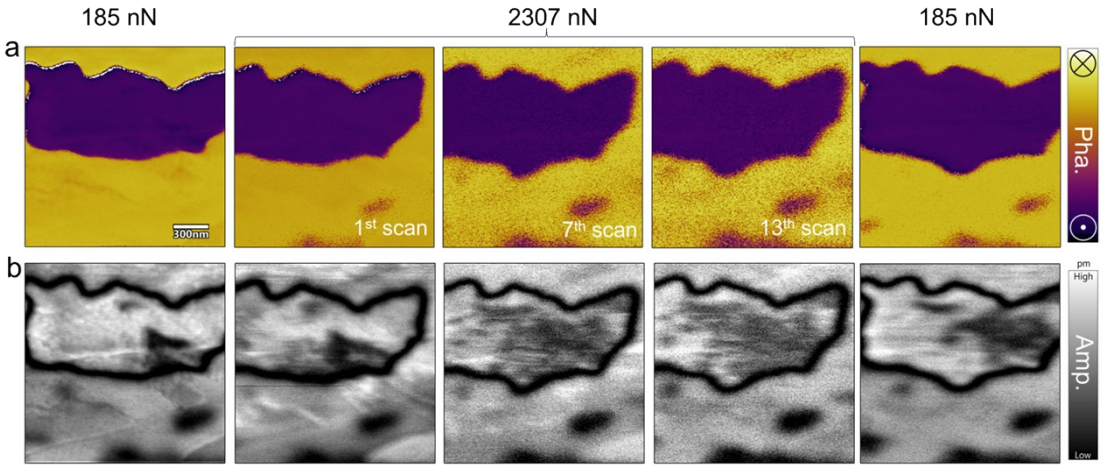

Figure S19. Anomalous mechanical polarization switching in 109-nm CIPS, which has been labelled by the black square in Figure S16. (a) Phase maps which contain both upward domains (purple) and downward domains (yellow) before high tip force, during high tip force, and after high tip force, (b) corresponding amplitude maps.

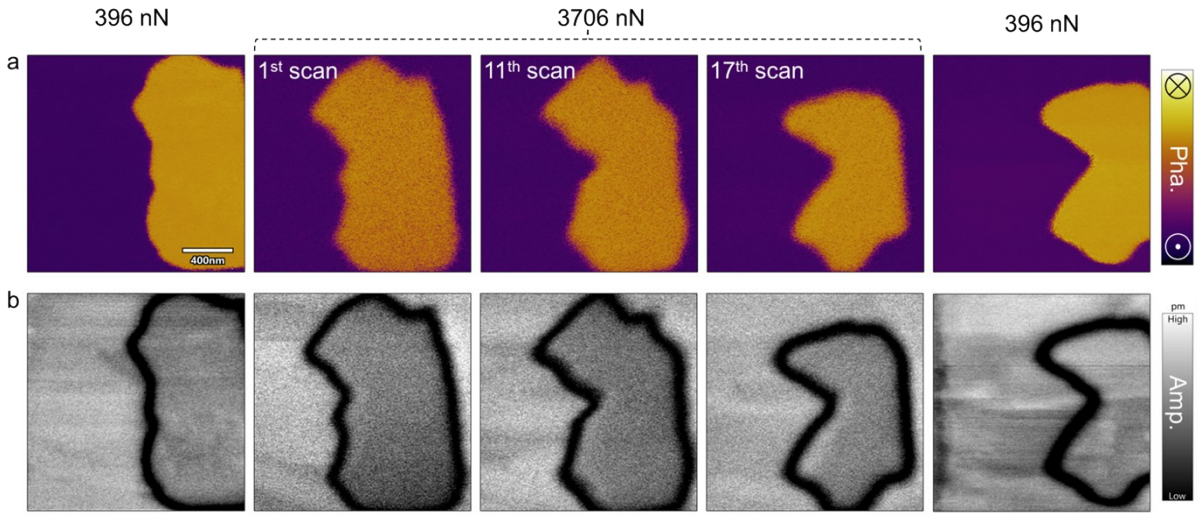

Figure S20. Anomalous mechanical polarization switching in electrical-writing domains. (a) Phase maps which contain both upward domains (purple, electrical-writing by +10 V) and downward domains (yellow, electrical-writing by -10 V) before high tip force, during high tip force, and after high tip force, (b) corresponding amplitude maps.

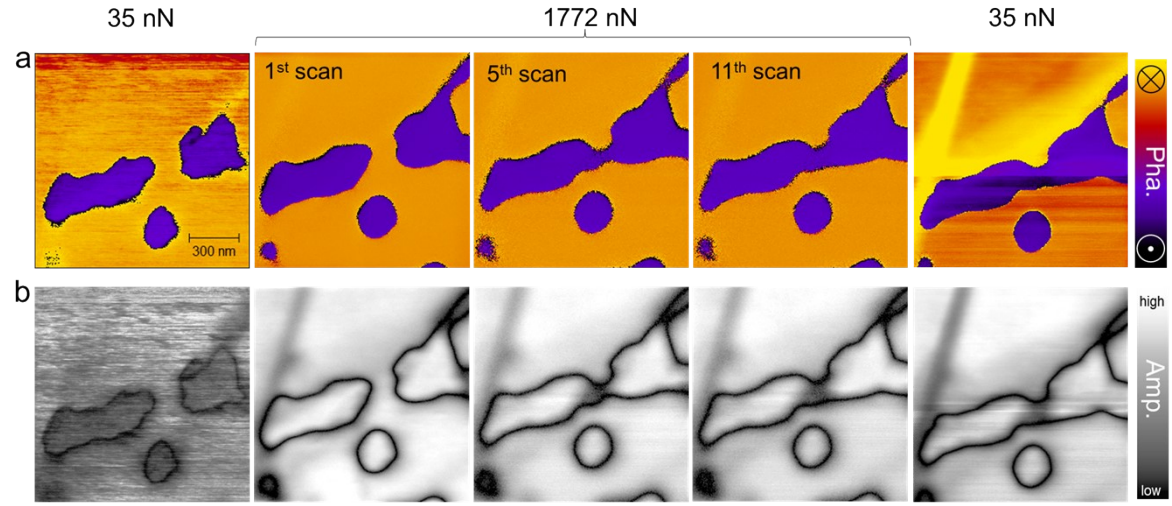

Figure S21. Mechanical polarization switching under N_2 atmosphere. (a) Phase maps which contain both upward domains (purple) and downward domains (yellow) before high tip force, during high tip force, and after high tip force, (b) corresponding amplitude maps.

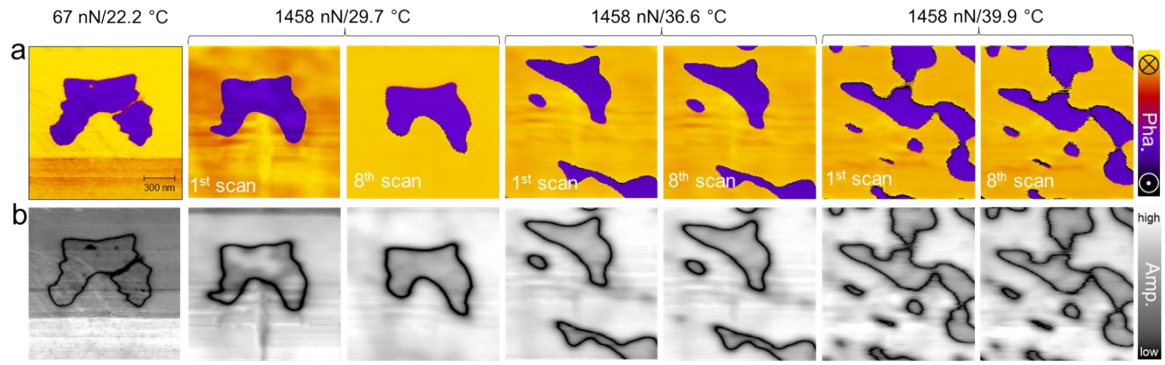

Figure S22. Mechanical polarization switching at different temperatures below the Curie temperature. (a) Phase maps which contain both upward domains (purple) and downward domains (yellow) before high tip force and during high tip force, (b) corresponding amplitude maps.

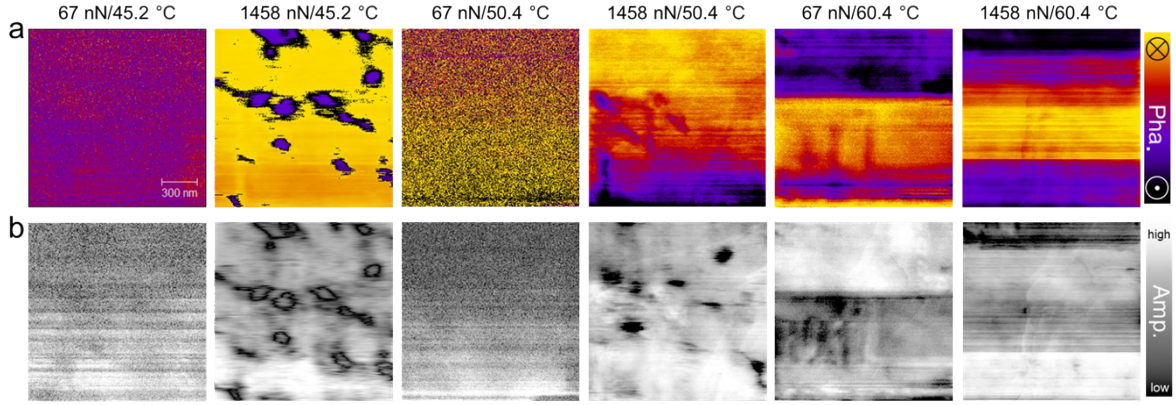

Figure S23. Mechanical polarization switching at different temperatures above the Curie temperature. (a) Phase maps which contain both upward domains (purple) and downward domains (yellow) before high tip force and during high tip force, (b) corresponding amplitude maps.